The Hexagonal Prism Shaped Cluster $W_2Ag_4S_8(AsPh_3)_4$: Synthesis, Crystal Structure, and Nonlinear Optical Properties

Genta Sakane,[†] Takashi Shibahare,[†] Hong W. Hou,[‡] Xin Q. Xin,[‡] and Shu Shi*[,§]

Department of Chemistry, Okayama University of Science, Okayama 700, Japan, State Key Laboratory of Coordination Chemistry, Department of Chemistry, Nanjing University, Nanjing 210008, China, and Optical Crystal Laboratory and Department of Chemical Engineering, National University of Singapore, Singapore 0511, Singapore

Received December 27, 1994[⊗]

$W_2S_8Ag_4(AsPh_3)_4$ was prepared by gently heating the solid-state reaction mixture of $(NH_4)_2WS_4$, AgBr, and $AsPh_3$. Its structure was determined by single-crystal X-ray diffraction. The compound crystallizes in the triclinic space group $P\bar{1}$ (No. 2), with $a = 12.440(2)$ Å, $b = 13.793(5)$ Å, $c = 11.513(3)$ Å, $\alpha = 96.41(2)°$, $\beta = 108.10(2)°$, $\gamma = 93.52(2)°$, $V = 1853.3(9)$ Å^3, and $Z = 2$; $R = 0.041$, $R_w = 0.060$. The structure can be described as a hexagonal prism shaped cage that consists of two identical butterfly shaped $WS_4(AgAsPh_3)_2$ segments. These segments are interconnected by four relatively long Ag–S bonds. The electronic spectrum, cyclic voltammogram, and X-ray photoelectron spectrum of the cluster were obtained. Nonlinear optical (NLO) properties of the cluster were studied with a 7-ns pulsed laser at 532 nm. The cluster exhibits both optical self-focusing and optical nonlinear absorption ($n_2^{eff} = 5.9 \times 10^{-17}$ m^2 W^{-1}; $\alpha_2^{eff} = 2.8 \times 10^{-9}$ m W^{-1}; examined in a 1.3×10^{-4} mol dm^{-3} acetonitrile solution). The corresponding effective third-order NLO susceptibility ($\chi^{(3)}_{eff}$) of the cluster is 1.7×10^{-10} esu. These nonlinear optical properties of the cluster are compared with those of butterfly shaped clusters and those of other known NLO materials.

Introduction

In today's optical data storage systems, laser light is normally focused to a diffraction-limited-sized spot in order to achieve high storage density. Tremendous technological interest in short-wavelength light was revived recently, following the first demonstration of 490-nm diode lasers fabricated from zinc selenide.[1,2] This is because the diameter of a diffraction-limited spot is directly proportional to the wavelength of the laser light used to produce the spot.

Great challenge remains in developing superior third-order nonlinear optical (NLO) materials which can utilize the short-wavelength laser light generated by the newly developed II–VI semiconductor diode laser to perform optical data processing. Both large values of third-order NLO susceptibility $\chi^{(3)}$ (or NLO refractive index n_2) and low linear absorptivity α_0 in this wavelength region are key criteria in screening new NLO materials. Currently, the most thoroughly studied third-order NLO materials (in terms of $\chi^{(3)}$ values) are inorganic semiconductors and conjugated organic polymers.[3–8] But both of the two types of the materials absorb light strongly in the short-wavelength region of the visible spectrum and are transparent only in the near-infrared.

In our recent search for NLO materials,[9–14] it was recognized that transition metal clusters may exhibit both large NLO effects and low extinction coefficients in the visible region if appropriate constituent elements, oxidation states, and cluster structures are selected. In this paper, we report the synthesis, crystal structure, linear spectrum, and NLO properties of a new cluster compound, $W_2Ag_4S_8(AsPPh_3)_4$.

Experimental Section

Reagents. The reagent $(NH_4)_2WS_4$ was prepared according to a literature method.[15] Other chemicals were of AR grade and were used without further purification.

Synthesis of $W_2Ag_4S_8(AsPh_3)_4$. A well-ground mixture of $(NH_4)_2WS_4$ (0.35 g, 1 mmol), AgBr (0.38 g, 2 mmol), and $AsPh_3$ (0.60 g, 2 mmol) was heated for 10 h at 100 °C under a pure nitrogen atmosphere. After extraction of the product with 10 mL of DMF and filtration of the deep brown extract, red crystals of $W_2Ag_4S_8(AsPh_3)_4$ were obtained 1 week later. Yield: 0.25 g. The compound is sparingly soluble in organic solvents such as CH_3COCH_3, CH_2Cl_2, CH_3CN, THF, and DMF. It shows characteristic infrared absorptions at 511 cm^{-1} for $\nu(W-S_t)$ and at 469 and 434 cm^{-1} for $\nu(W-S_{br})$. Anal. Calcd for $C_{72}H_{60}Ag_4As_4S_8W_2$: C, 37.93; H, 2.64; Found: C, 37.51; H, 2.72.

Instruments for Characterization. The infrared spectrum was recorded on a Fourier Nicolet FT-170SX spectrophotometer with pressed KBr pellets, the electronic spectrum was taken on a Hitachi UV-3410, and carbon and hydrogen analyses were performed on a PE 240C elemental analyzer. The cyclic voltammogram was recorded with

* To whom correspondence should be addressed.
† Okayama University of Science.
‡ Nanjing University.
§ National University of Singapore.
⊗ Abstract published in *Advance ACS Abstracts,* August 15, 1995.

(1) Haase, M. A.; Qiu, J.; DePuydt, J. M.; Cheng, H. *Appl. Phys. Lett.* **1991**, *59*, 1272.
(2) Neumark, G. F.; Park, R. M.; DePuydt, J. M. *Phys. Today* **1994**, *47* (6), 26.
(3) Chemla, D. S.; Zyss, J. *Nonlinear Optical Properties of Organic Molecules and Crystals*; Academic: New York, 1987; Vol. 2.
(4) Prasad, P. N.; Williams, D. *Introduction to Nonlinear Optical Effects in Molecules & Polymers*; John Wiley & Sons: New York, 1991.
(5) Bredas, J. L.; Adant, C.; Tackx, P.; Persoons, A. *Chem. Rev.* **1994**, *94*, 243.
(6) Nakanishi, H. *Nonlinear Opt.* **1991**, *1*, 223.
(7) Marder, S. R.; Sohn, J. E.; Stucky, G. D., Eds. *Materials for Nonlinear Optics, Chemical Perspectives*; American Chemical Society: Washington, DC, 1991.
(8) Sheik-Bahae, M.; Hutchings, D. C.; Hagan, D. J.; Van Stryland, E. W. *IEEE J. Quant. Electron* **1991**, *27*, 1296.
(9) Shi, S.; Ji, W.; Tang, S. H.; Lang, J. P.; Xin, X. Q. *J. Am. Chem. Soc.* **1994**, *116*, 3615.
(10) Shi, S.; Ji, W.; Lang, J. P.; Xin, X. Q. *J. Phys. Chem.* **1994**, *98*, 3570.
(11) Shi, S.; Ji, W.; Xie, W.; Chong, T. C.; Zeng, H. C.; Lang, J. P.; Xin, X. Q. *Mater. Chem. Phys.* **1995**, *39*, 298.
(12) Shi, S.; Ji, W.; Xin, X. Q. *J. Phys. Chem.* **1995**, *99*, 894.
(13) Hou, H. W.; Xin, X. Q.; Liu, J.; Chen, M. Q.; Shi, S. *J. Chem. Soc., Dalton Trans.* **1994**, 3211.
(14) Hou, H. W.; Ye, X. R.; Liu, J.; Chen, M. Q.; Shi, S. *Chem. Mater.* **1995**, *7*, 472.
(15) McDonald, J. W.; Frieson, G. D.; Rosenhein, L. D.; Newton, W. E. *Inorg. Chim. Acta* **1983**, *72*, 205.

0020-1669/95/1334-4785$09.00/0

Table 1. Crystal Parameters for the $W_2Ag_4S_8(AsPh_3)_4$ Cluster[a]

chem formula: $C_{36}H_{30}Ag_2As_2S_4W$	fw: 1140.30
$a = 12.440(2)$ Å	space group: $P\bar{1}$ (No. 2)
$b = 13.793(5)$ Å	$T = 12$ °C
$c = 11.513(3)$ Å	$\lambda = 0.710\,69$ Å (Mo Kα)
$\alpha = 96.41(2)°$	$\rho_{calc} = 2.024$ g/cm^3
$\beta = 108.10(2)°$	μ(Mo Kα) = 61.56 cm^{-1}
$\gamma = 93.52(2)°$	$R(F_o) = 0.041$
$V = 1856.3(9)$ Å^3	$R_w(F_o) = 0.060$
$Z = 2$	

[a] Diffractometer Rigaku AFC6S; scan type ω; $(2\theta)_{max} = 59.9°$; $F(000) = 1088$; number of total reflections = 3563; number of unique reflections = 3385. Corrections: Lorentz–polarization and absorption. Definitions: $R = \sum||F_o| - |F_c||/\sum|F_o|$; $R_w = [\sum w(|F_o| - |F_c|)^2/\sum wF_o^2]^{1/2}$; $w = 1/\sigma^2(F_o) = 4F_o^2/\sigma^2(F_o^2)$; $\sigma^2(F_o^2) = [S^2(C + R^2B) + (pF_o^2)^2]/(Lp)^2$; S = scan rate; C = total integrated peak count; R = ratio of scan time to background counting time; B = total background counting; p = p-factor; Lp = Lorentz–polarization factor.

a PN Model 270 electrochemical analyzer. The measurement was made in a CH_3CN solution containing 10^{-1} mol dm^{-3} Et_4NClO_4 as supporting electrolyte, using platinum as the working electrode under a nitrogen atmosphere. X-ray photoelectron spectral (XPS) data were obtained with an ESCALAB MK-II electron spectrometer.

Crystal Structure Analysis. The molecular structure of $W_2Ag_4S_8(AsPh_3)_4$ was determined by a single-crystal X-ray diffraction data analysis. The crystal is stable toward oxygen and moisture. The diffraction data collection was carried out at 12 °C and covered $\pm h,\pm k,\pm l$ octants. The range of transmission factors was calculated to be 0.8636–1.3924. A summary of the crystal parameters and details concerning the diffraction intensity data collection is given in Table 1. The structure was solved with TEXSAN crystallographic software using a combination of direct methods and Fourier techniques. The non-hydrogen atoms were refined anisotropically. The scattering factors F_0 F', and F'' were taken from refs 16 and 17. The final cycle of full-matrix least-squares refinement was based on 3101 observed reflections ($I > 3.00\sigma(I)$) and 406 variables. It converged with $R = 0.041$ and $R_w = 0.060$.

Nonlinear Optical Measurements. An acetonitrile solution of the title cluster (1.3×10^{-4} mol dm^{-3}, limited by solubility) was placed in a 1-mm quartz cuvette for NLO measurements. Its nonlinear refraction and nonlinear absorption were measured with a linearly polarized laser light ($\lambda = 532$ nm; pulse width = 7 ns) generated from a Q-switched and frequency-doubled Nd-YAG laser. The spatial profiles of the optical pulses were nearly Gaussian after passing through a spatial filter. The laser beam was focused with a 25-cm focal-length focusing mirror. The radius of the beam circumference was measured to be 30 ± 5 μm (half-width at $1/e^2$ maximum in irradiance). The incident and transmitted pulse energy were measured simultaneously by two energy detectors (Laser Precision RjP-735) which were linked to a computer by an IEEE interface. The interval between the laser pulses was chosen to be ~5 s for operational convenience and controlled by the computer. The NLO properties of the samples were manifested by moving the samples along the axis of the incident beam (Z-direction) with respect to the focal point and with incident laser irradiance kept constant (Z-scan method).[18] An aperture of 0.5 mm radius was placed in front of the detector measuring transmitted energy when assessment of laser beam distortion was needed. Reliability of the measuring system was tested with CS_2. An n_2 value of $(2.0 \pm 0.8) \times 10^{-11}$ esu was obtained at 532 nm for CS_2, which is in good agreement with the reported value of $n_2 = 1.2 \times 10^{-11}$ esu.[19]

Results and Discussion

Description of Structure. The molecular structure of the title compound is given in Figure 1. Figure 2 shows the packing

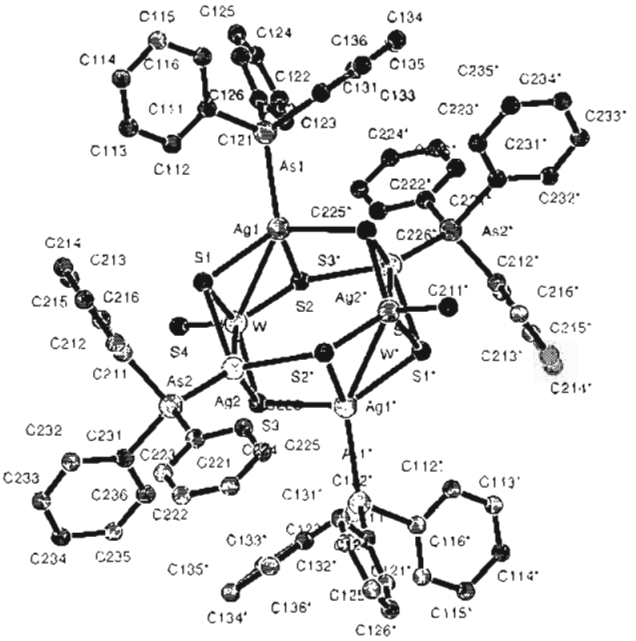

Figure 1. Crystal structure of $W_2Ag_4S_8(AsPh_3)_4$.

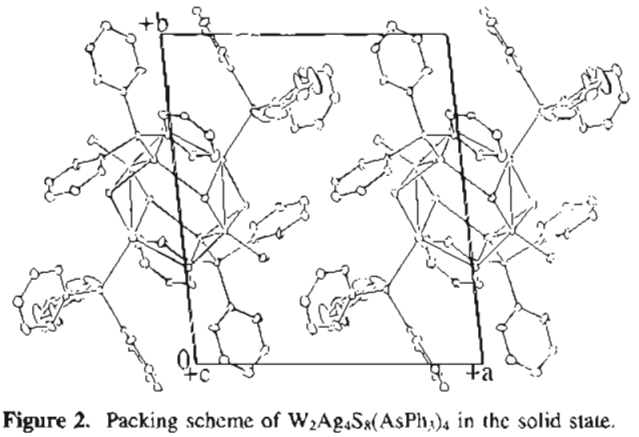

Figure 2. Packing scheme of $W_2Ag_4S_8(AsPh_3)_4$ in the solid state.

scheme of the molecules in the unit cell. Atomic coordinates and B_{eq} values are presented in Table 2. Selected bond lengths and bond angles are collected in Tables 3 and 4, respectively. The core of the cluster, $W_2Ag_4S_8$, can be described either as a cage that consists of two fused six-member W–S–Ag–S–Ag–S rings or as a hexagonal cage that consists of two identical butterfly shaped $WAg_2S_4(AsPh_3)_2$ segments. The latter description is more instructive from a synthetic point of view and justified by the fact that the Ag(1)–S(3)* (or Ag(2)–S(2)*) distance is over 0.11 Å longer than the Ag(1)–S(2) (or Ag(2)–S(3)) distance. Both the hexagonal prism ("dimer of butterfly") structure of $W_2Ag_4S_8(AsPh_3)_4$ and the structure of a butterfly shaped cluster $WOS_3Cu_2(PPh_3)_4$ are illustrated as follows:

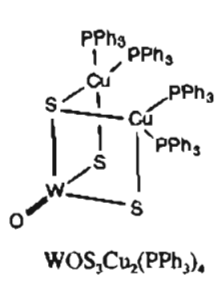

$WOS_3Cu_2(PPh_3)_4$

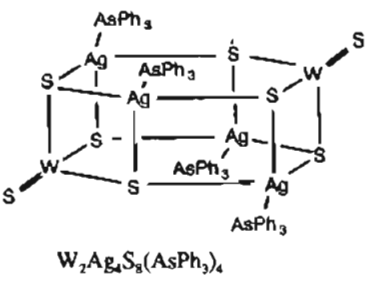

$W_2Ag_4S_8(AsPh_3)_4$

Unlike the Cu atoms in $WOS_3Cu_2(PPh_3)_4$, which adopt normal

(16) Cromer, D. T.; Waber, J. T. *International Tables for X-ray Crystallography*; The Kynoch Press: Birmingham, England, 1974; Vol. IV.
(17) Creagh, D. C.; McAuley, W. J. In *International Tables for X-ray Crystallography*; Wilson, A. J. C., Ed.; Kluwer: Boston, 1992; Vol. C.
(18) Sheik-Bahae, M.; Said, A. A.; Van Stryland, E. W. *Opt. Lett.* **1989**, *14*, 955.
(19) Sheik-Bahae, M.; Said, A. A.; Wei, T. H.; Hagan, D. J.; Van Stryland, E. W. *IEEE J. Quant. Electron* **1990**, *26*, 760.

Table 2. Atomic Coordinates and B_{eq} Values for the $W_2Ag_4S_8(AsPh_3)_4$ Cluster

atom	x	y	z	B_{eq},[a] Å^2
W	−0.15621(4)	−0.40131(3)	−0.10789(4)	1.91(2)
Ag(1)	−0.17148(9)	−0.61803(7)	−0.11085(9)	3.37(3)
Ag(2)	−0.06627(8)	−0.38037(8)	0.16917(9)	3.23(3)
As(1)	−0.3063(1)	−0.77381(10)	−0.1863(1)	2.80(4)
As(2)	−0.1118(1)	−0.30907(9)	0.3567(1)	2.39(3)
S(1)	−0.2377(3)	−0.4828(2)	0.0078(3)	2.84(9)
S(2)	−0.0992(3)	−0.5013(2)	−0.2364(3)	2.83(9)
S(3)	−0.0135(3)	−0.2918(2)	0.0072(3)	2.60(8)
S(4)	−0.2791(3)	−0.3209(3)	−0.2190(3)	3.9(1)
C(111)	−0.425(1)	−0.7917(10)	−0.111(1)	3.2(4)
C(112)	−0.440(1)	−0.715(1)	−0.034(1)	3.8(4)
C(113)	−0.526(1)	−0.727(1)	0.021(2)	5.2(5)
C(114)	−0.591(1)	−0.809(1)	−0.001(2)	5.6(6)
C(115)	−0.578(1)	−0.891(1)	−0.078(2)	6.3(6)
C(116)	−0.490(1)	−0.883(1)	−0.131(1)	5.0(5)
C(211)	−0.2494(9)	−0.3775(9)	0.367(1)	2.6(3)
C(212)	−0.252(1)	−0.417(1)	0.472(1)	3.6(4)
C(213)	−0.351(1)	−0.476(1)	0.471(2)	5.4(5)
C(214)	−0.441(1)	−0.494(1)	0.361(2)	5.2(5)
C(215)	−0.439(1)	−0.451(1)	0.257(1)	4.4(5)
C(216)	−0.341(1)	−0.396(1)	0.257(1)	4.3(4)

[a] $B_{eq} = (8\pi/3)[U_{11}(aa^*)^2 + U_{22}(bb^*)^2 + U_{33}(cc^*)^2 + 2U_{12}aa^*bb^* \cos\gamma + 2U_{13}aa^*cc^* \cos\beta + 2U_{23}bb^*cc^* \cos\alpha]$.

Table 3. Selected Bond Lengths (Å) of the $W_2Ag_4S_8(AsPh_3)_4$ Cluster

W−Ag(1)	2.979(1)	W−Ag(2)	3.008(1)
W−S(1)	2.258(3)	W−S(2)	2.216(3)
W−S(3)	2.225(3)	W−S(4)	2.215(3)
Ag(1)−As(1)	2.533(2)	Ag(1)−S(1)	2.519(3)
Ag(1)−S(2)	2.576(4)	Ag(1)−S(3)	2.691(3)
Ag(2)−As(2)	2.511(2)	Ag(2)−S(1)	2.565(3)
Ag(2)−S(2)	2.684(3)	Ag(2)−S(3)	2.563(3)
As(1)−C(111)	1.94(1)	As(1)−C(121)	1.95(1)
As(1)−C(131)	1.95(1)	As(2)−C(211)	1.95(1)
As(2)−C(221)	1.95(1)	As(2)−C(231)	1.93(1)
C(111)−C(112)	1.37(2)	C(111)−C(116)	1.41(2)
C(112)−C(113)	1.41(2)	C(113)−C(114)	1.31(2)
C(114)−C(115)	1.41(2)	C(115)−C(116)	1.42(2)

Table 4. Selected Bond Angles (deg) of the $W_2Ag_4S_8(AsPh_3)_4$ Cluster

Ag(1)−W−Ag(2)	88.15(4)	Ag(1)−W−S(1)	55.46(8)
Ag(1)−W−S(2)	57.23(9)	Ag(1)−W−S(3)	127.21(9)
Ag(1)−W−S(4)	126.5(1)	Ag(2)−W−S(1)	56.13(8)
Ag(2)−W−S(2)	125.73(9)	Ag(2)−W−S(3)	56.29(9)
Ag(2)−W−S(4)	127.8(1)	S(1)−W−S(2)	112.5(1)
S(1)−W−S(3)	112.1(1)	S(1)−W−S(4)	108.6(1)
S(2)−W−S(3)	110.5(1)	S(2)−W−S(4)	106.5(1)
S(3)−W−S(4)	106.3(1)	W−Ag(1)−As(1)	143.55(5)
W−Ag(1)−S(1)	47.60(8)	W−Ag(1)−S(2)	46.31(7)
W−Ag(1)−S(3)	121.06(8)	As(1)−Ag(1)−S(1)	115.35(9)
As(1)−Ag(1)−S(2)	129.22(9)	As(1)−Ag(1)−S(3)	95.37(8)
S(1)−Ag(1)−S(2)	93.8(1)	S(1)−Ag(1)−S(3)	122.5(1)
S(2)−Ag(1)−S(3)	102.8(1)	W−Ag(2)−As(2)	141.01(5)
Ag(1)−As(1)−C(111)	117.4(4)	Ag(2)−As(2)−C(211)	111.1(3)
W−S(1)−Ag(1)	76.94(10)	W−S(2)−Ag(1)	76.5(1)
W−S(3)−Ag(1)	110.4(1)	Ag(1)−S(1)−Ag(2)	110.0(1)
Ag(1)−S(2)−Ag(2)	75.74(9)	Ag(1)−S(3)−Ag(2)	75.84(9)

tetrahedral coordination, the Ag atoms in $W_2Ag_4S_8(AsPh_3)_4$ adopt quite distorted tetrahedral geometry (three S atoms and one $AsPh_3$ ligand), with bond angles ranging from 93.8(1) to 129.0(9)°.

In $W_2Ag_4S_8(AsPh_3)_4$, a crystallographic center of symmetry is located in the center of the cluster. The two identical $WAg_2S_4(AsPh_3)_2$ fragments are related to each other through the inversion center. The terminal positions around the Ag atoms are occupied by the $AsPh_3$ ligands. The W atom is tetrahedrally coordinated by four S atoms (with S−W−S angles being 106.3(1)−112.5(1)°). The terminal W−S bond length of 2.125(3) Å is similar to that of 2.165 Å in $(NH_4)_2WS_4$.[20] The bond lengths from W to bridging S (bridging to one W and two Ag atoms) range from 2.216(3) to 2.258(3) Å and are close to those of related compounds.[21−23]

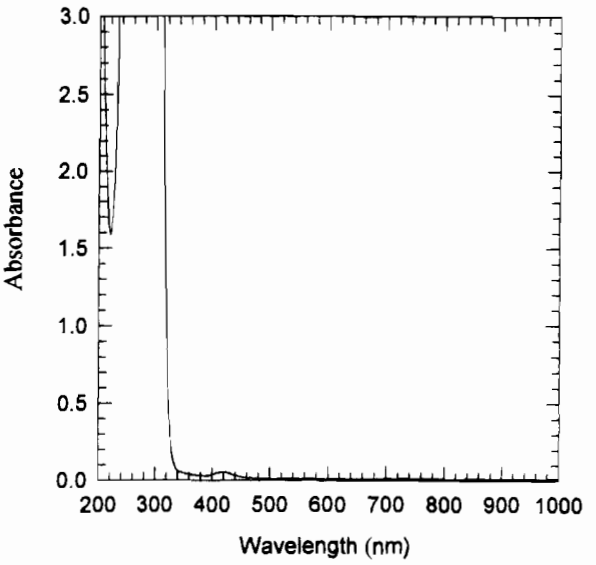

Figure 3. Electronic spectrum of $W_2Ag_4S_8(AsPh_3)_4$ (9.1×10^{-5} mol dm^{-3}) in acetonitrile. Optical path is 1 mm.

Electronic Spectrum. The wide transparent window of the WS_4^{2-} group in the visible and near-infrared regions[15] and the closed d-shell configuration of Ag(I) are purposely combined in designing and synthesizing the title cluster to minimize its linear optical absorption and maximize its third-order nonlinear optical figures of merit,[24] $n_2I/(\alpha_0\lambda)$ where n_2, I, and λ are the nonlinear refractive index, the on-axis irradiance, and the wavelength of the incident light. The dominant features of the electronic spectrum of $W_2S_8Ag_4(AsPh_3)_4$ are its weak absorption between 340 and 460 nm and practically no absorption from 460 to 1000 nm.

Nonlinear Optical Properties. We discovered recently that butterfly shaped clusters $MCu_2OS_3(PPh_3)_n$ (M = Mo, n = 3; M = W, n = 4) exhibit superior effective third-order NLO properties.[25] One wonders, naturally, what NLO property a "dimer" of such butterfly clusters will exhibit. This paper reports that the cluster $W_2Ag_4S_8(AsPh_3)_4$ exhibits both strong NLO absorption and strong NLO refraction.

Nonlinear Optical Absorption. The nonlinear absorption component of $W_2Ag_4S_8(AsPh_3)_4$ was evaluated by Z-scan experiment under an open-aperture configuration (Figure 4a). Although the detailed mechanism is still unknown, it is interesting to note that the NLO absorption data obtained under the conditions used in this study (maximum incident irradiance $I(Z = 0) = 1.1 \times 10^{12}$ W m^{-2}) can be well described by eqs 1 and 2,which are derived to describe a third-order NLO process,[19]

$$T(Z) = \frac{1}{\sqrt{\pi}q(Z)}\int_{-\infty}^{\infty}\ln[1 + q(Z)]e^{-\tau^2}\,d\tau \qquad (1)$$

$$q(Z) = \alpha_2^{\text{eff}}\, I(Z)\frac{1 - e^{-\alpha_0 L}}{\alpha_0} \qquad (2)$$

(20) Sarvari, K. *Acta Crystallogr.* **1963**, *16*, 719.
(21) Meuller, A.; Bogge, H.; Koniger-Ahlborn, E.; Hellmann, W. *Inorg. Chem.* **1979**, *18*, 2031.
(22) Meuller, A.; Bogge, H.; Koniger-Ahlborn, E. *J. Chem. Soc., Chem. Commun.* **1978**, 793.
(23) Stalick, J. K.; Siedle, A.; Mighell, A. D.; Hubbard, C. *J. Am. Chem. Soc.* **1979**, *101*, 2903.
(24) Boyd, G. T. *J. Opt. Soc. Am. B* **1989**, *6*, 685.
(25) Shi, S.; Hou, H. W.; Xin, X. Q. *J. Phys. Chem.* **1995**, *99*, 4050.

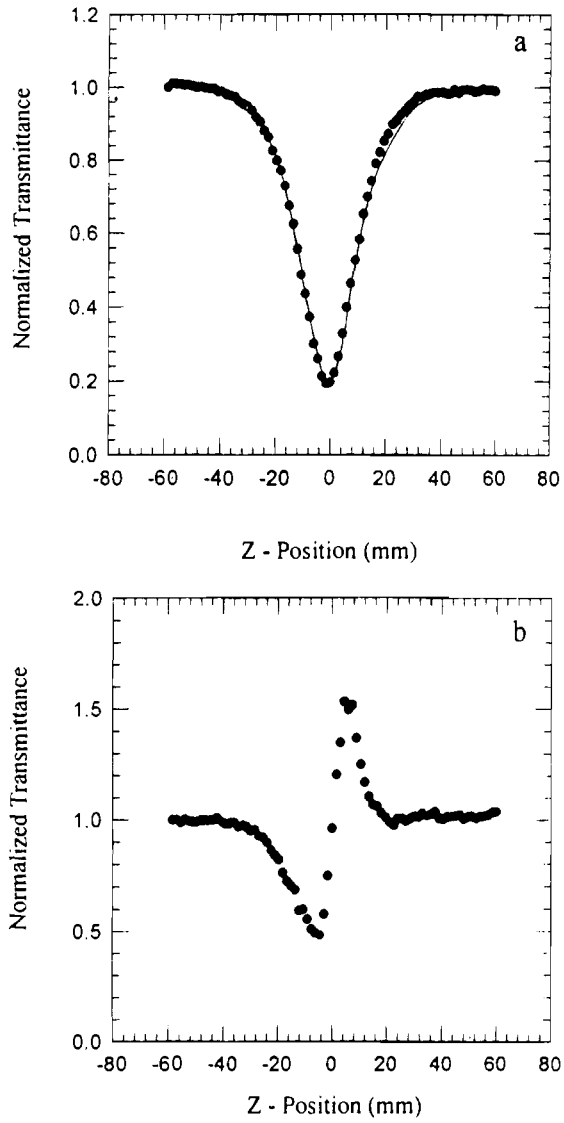

Figure 4. *Z*-Scan data (filled circles) for 1.3×10^{-4} mol dm^{-3} $W_2Ag_4S_8(AsPh_3)_4$, at 532 nm with $I(Z=0)$ being 1.1×10^{12} W m^{-2}. (a) Data were collected under the open-aperture configuration showing NLO absorption. The solid curve is a theoretical fit based on eqs 1 and 2, where $\alpha_0 = 1.1 \times 10$ m^{-1} (at 532 nm) and $L = 1.0 \times 10^{-3}$ m. (b) Data were obtained by dividing the normalized *Z*-scan data obtained under the closed-aperture configuration by the normalized *Z*-scan data in (a). This plot shows the self-focusing effect of the cluster.

where α_0 and α_2^{eff} are linear and effective third-order NLO absorptivities, respectively. Light transmittance (T) is a function of the sample's *Z*-position (against focal point $Z = 0$). The best fit of the theoretical curve (the solid curve in Figure 4a) to the experimental data (filled circles) was obtained with an α_2^{eff} value of 2.8×10^{-9} m W^{-1}. A control experiment showed that photodamage of the quartz cuvette did not occur to any detectable extent under the experimental conditions. It is therefore not responsible for the observed NLO effect. The damage threshold of the quartz cuvette was measured to be 1.5×10^{13} W m^2. Bubble formation due to local heating can also be ruled out under the conditions used.

It should be pointed out that an excited state absorption (two consecutive one-photon absorptions) has been discovered to be responsible for the measured NLO effects of related clusters.[26-28] Such consecutive one-photon absorptions may behave very similarly to a genuine two-photon absorption under the influence of a nanosecond laser pulse. The existing experimental data are insufficient to identify the relative contributions of these two mechanisms. The observed nonlinear absorption should be viewed only as an effectively third-order process at this point.

Nonlinear Optical Refraction. The nonlinear refractive properties of the cluster $W_2Ag_4S_8(AsPh_3)_4$ were assessed by dividing the normalized *Z*-scan data obtained under the closed-aperture configuration by the normalized *Z*-scan data obtained under the open-aperture configuration (Figure 4b). This procedure extracts information of NLO refraction from a raw data set containing mixed information of both refraction and absorption.[19] The valley/peak pattern of the corrected transmittance curve so obtained shows characteristic self-focusing behavior of propagating light in the sample.

An effective third-order nonlinear refractive index n_2^{eff} (m^2 W^{-1}) can be derived from the difference between normalized transmittance values at valley and peak positions, ΔT_{v-p}, by eq 3, where n_2^{eff} is the effective nonlinear refractive index. With

$$n_2^{eff} = \frac{\lambda \alpha_0}{0.812\pi I(1 - e^{-\alpha_0 L})} \Delta T_{v-p} \qquad (3)$$

measured values of $\Delta T_{v-p} = 1.0$, $\alpha_0 = 1.1 \times 10^1$ m^{-1}, and $L = 1.0 \times 10^{-3}$, the n_2^{eff} value was calculated to be 5.9×10^{-17} m^2 W^{-1}.

The very fact that an acetonitrile solution of $W_2Ag_4S_8(AsPh_3)_4$ causes self-focusing of the propagating light rules out solution thermal effects as being responsible for the observed NLO effects because acetonitrile is known to have a negative value of dn/dT (-4.5×10^{-4} K^{-1}).[29] This is consistent with our earlier results for related Mo(W)−Cu(Ag)−S clusters.[9-14,25]

Comparison with Known NLO Materials. On the basis of the above-mentioned results, we conclude that the observed NLO properties of $W_2Ag_4S_8(AsPh_3)_4$ are of electronic origin and qualitatively resemble those of the butterfly shaped clusters. Listed in Table 5 are values of selected third-order NLO parameters of $W_2Ag_4S_8(AsPh_3)_4$ and the butterfly shaped clusters along with those of known inorganic semiconductors and conjugated organic polymers.

Inorganic semiconductors have attracted attention since the 1970s because relatively large $\chi^{(3)}$ values have been detected in this group of materials: for example, 4.8×10^{-11} esu for GaAs and 4×10^{-10} esu for Ge.[30] A common problem with many inorganic semiconductors is their large linear absorption (α_0) and hence small figure of merit $\chi^{(3)}/\alpha_0$ in the visible region (especially the blue-green region) of spectrum.

Third-order NLO materials are exploited for applications in optical data processing. Since all the data processed have to be stored, it is prudent to exploit new third-order NLO materials that can process optical signals carried by short-wavelength light. This is because the processed optical signals can then be sent directly to optical data storage media without frequency conversion. From the optical data storage point of view, the shorter the operation wavelength, the higher the optical data storage density.

Great efforts have gone into developing discrete organic NLO materials since the 1980s to achieve shorter cutoff wavelengths. Some success was achieved with conjugated organic polymeric materials, such as members of the poly(diacetylene) and poly-

(26) Ji, W.; Du, H. J.; Shi, S. *J. Opt. Soc. Am.* **1995**, *12*, 876.
(27) Ji, W.; Xie, W.; Tang, S. H.; Shi, S. *Mater. Phys. Chem.*, in press.
(28) Ji, W.; Shi, S.; Du, H. J.; Ge, P.; Xin, X. Q. *J. Phys. Chem.*, in press.
(29) Riddick, J. A.; Bunger, W. B.; Sakano, T. K. *Organic Solvents: Physical Properties and Method of Purification*, 4th ed.; John Wiley & Sons: New York, 1986.
(30) Kobayashi, T. *IEICE Trans. Fundam.* **1992**, *E75-A*, 38.

Table 5. Selected Third-Order NLO Parameters

material	n_2 (cm^2 W^{-1})	α_0 (cm^{-1})	$\chi^{(3)}$ (esu)	concn (mol dm^{-3})	λ (nm)	ref
			Semiconductors			
GaAs	$<-3 \times 10^{-13}$	1.0	4.8×10^{-11}	neat	1064	5, 30
AlGaAs (790 nm)	-4×10^{-12}	18		neat	810	5
AlGaAs (750 nm)	2×10^{-13}	0.1		neat	1560	5
			Organic Polymers			
PDA-PTS	5×10^{-12}			neat	1064	32
			8.5×10^{-10}	neat	700	6
PDA-4BCMU	5×10^{-14}	<0.2	1.8×10^{-10}	neat	1310	5, 6
	4.8×10^{-14}	0.06		neat	1319	33
DANS	8×10^{-14}	<0.2		neat	1060	5
PA			5.0×10^{-10}	neat	1064	6
			Inorganic Clusters			
$WCu_2OS_3(PPh_3)_4$	8×10^{-14}	0.3	2.0×10^{-11}	1.2×10^{-4}	532	25
$W_2Ag_4S_8(AsPh_3)_4$	6×10^{-13}	0.1	2.0×10^{-10}	1.3×10^{-4}	532	this work

(thiophene) families, where reasonably low α_0 values and large third-order NLO susceptibilities $\chi^{(3)}$ of $10^{-11}-5 \times 10^{-10}$ esu were detected in the near-infrared region, as shown in Table 5. Unfortunately, the overall $\chi^{(3)}/\alpha_0$ values in the visible region are still too low. The frustrating fact is that the intensive search for organic materials with larger $\chi^{(3)}$ values and shorter cutoff wavelengths has proven essentially futile in the last decade.

Inorganic clusters uniquely combine the merits of inorganic semiconductors and organic molecules. They resemble organic molecules in that they are discrete molecules. Both the skeleton atoms and peripheral ligands can be changed to achieve desired structures and to tailor linear optical properties. On the other hand, they resemble inorganic semiconductors in having large numbers of heavy atoms. These heavy atoms introduce large numbers of excited states positioned close to the ground state and therefore enhance the NLO performance of the materials.

The cluster $W_2Ag_4S_8(AsPh_3)_4$ serves as an example demonstrating the great potential of inorganic clusters in NLO applications. From the α_2^{eff} and n_2^{eff} values, the effective third-order susceptibility $\chi^{(3)}_{eff}$ can be calculated according to eq 4.

$$|\chi^{(3)}_{eff}| = \sqrt{\left|\frac{9 \times 10^8 \epsilon_0 n_0^2 c^2}{4\pi\omega}\alpha_2^{eff}\right|^2 + \left|\frac{cn_0^2}{80\pi}n_2^{eff}\right|^2} \quad (4)$$

For a 1.3×10^{-4} mol dm^{-3} acetonitrile solution of $W_2Ag_4S_8(AsPh_3)_4$, the $\chi^{(3)}_{eff}$ value was calculated to be 1.7×10^{-10} esu. (This corresponds to an effective hyperpolarizability γ_{eff} of 7.2×10^{-28} esu for the cluster.) This value is already close to those of well-known NLO semiconductors and organic polymers (see Table 5).

It is also noted that while the $\chi^{(3)}$ values of $10^{-11}-5 \times 10^{-10}$ esu were achieved by neat poly(thiophenes) and poly(diacetylenes), the $\chi^{(3)}_{eff}$ value of 1.7×10^{-10} esu was achieved by 1.3×10^{-4} mol dm^{-3} $W_2Ag_4S_8(AsPh_3)_4$ in solution (limited by its solubility). In other words, the inorganic cluster promises an increase of 4−5 orders of magnitude in the $\chi^{(3)}_{eff}$ value (from the current level of 10^{-10} esu) provided that the solubility of the cluster in a solution (or in a transparent host polymer) can be increased by the same magnitude.

Cyclic Voltammogram and X-ray Photoelectron Spectrum. Two separate lines of experiments were conducted: cyclic voltammetry and X-ray photoelectron spectroscopy. The cyclic voltammogram of the title cluster was obtained in CH_3CN in the hope that the NLO properties of the reduction or oxidation product of the cluster can later be studied and compared with the NLO properties of $W_2S_8Ag_4(AsPh_3)_4$ itself. One of the advantages of using inorganic clusters as NLO chromophores is that they are often stable in more than one oxidation state (unlike most of organic aromatic chromophores). The total charge of a cluster can also be changed to adjust its polarizability and the energies of relevant electronic states. Fortunately, unlike those of many other W(Mo)−Ag(Cu)−S clusters studied[13,14] where the reduction or oxidation products are unstable, the cyclic voltammogram of $W_2Ag_4S_8(AsPh_3)_4$ does contain a reversible redox wave ($E_{pa1} = -0.10$ V, $E_{pc1} = -0.08$ V) in addition to two irreversible redox waves ($E_{pa2} = -1.25$ V and $E_{pa3} = -1.75$ V). By comparison with the cyclic voltammograms of other W(Mo)−Ag(Cu)−S clusters,[13,14,31] we tentatively assign the E_{pa1}/E_{pc1} pair to Ag and the E_{pa2} and E_{pa3} waves to W.

Table 6. Binding Energies (eV) and Formal Oxidation States of Several Elements in $W_2Ag_4S_8(AsPh_3)_4$

		binding energy	oxidn state			binding energy	oxidn state
W	$4f_{7/2}$	33.60	+6	As	3d	42.90	+3
	$4f_{5/2}$	35.20		S	2p	161.80	−2
Ag	$3d_{5/2}$	368.60	+1				
	$3d_{3/2}$	374.70					

The formal oxidation state of W in the reagent WS_4^{2-} is +6 and of Ag in the reagent AgBr is +1. In the $W_2Ag_4S_8(AsPh_3)_4$ cluster, W ions are expected to have strong interactions with Ag through $W(S)_2Ag$. It is important to accumulate a set of data that quantize the electron density distribution of structurally related clusters so that possible correlation can be gradually revealed between cluster structures and their NLO properties in the future. The XPS measurement makes it possible to deduce the electron density distribution of a cluster through the changes in binding energy and to assign formal oxidation states to individual constituent elements. Table 6 lists the measured binding energies of selected elements in $W_2Ag_4S_8(AsPh_3)_4$ along with the corresponding assignments of their formal oxidation states. These assignments are confirmed by the bond lengths and angles derived from X-ray diffraction data.

Supporting Information Available: Descriptions of X-ray diffraction data collection and refinement procedures and tables of cell parameters, atomic coordinates, bond distances, bond angles, torsion angles, and anisotropic displacement parameters, along with all of the corresponding estimated standard deviations (13 pages). Ordering information is given on any current masthead page.

IC941471N

(31) Chen, Z. R.; Hou, H. W.; Xin, X. Q.; Yu, K. B.; Shi, S. *J. Phys. Chem.* **1995**, *99*, 8717.
(32) Lawrence, B. L.; Cha, M.; Torruellas, W. E.; Stegeman, G. I.; Etenmad, S.; Baker, G.; Kajzar, F. *Appl. Phys. Lett.* **1994**, *64*, 2773.
(33) Rochford, K. B.; Zanoni, R.; Stegeman, G. I.; Krug, W.; Miao, E.; Beranek, M. W. *IEEE J. Quant. Electron* **1992**, *28*, 2044.